Numerical Resolution Requirements for Narrow Channel Detonation Simulations

Milin Martin[a], Ashwath Sethu Venkataraman[a], Elaine S Oran[a], Hoden Farah[b]
[a]Department of Aerospace Engineering, Texas A&M University, College Station, Texas, USA
[b]Emerson Process Management Regulator Technologies Inc., Mckinney, Texas, USA

1 Introduction

A substantial amount of numerical work has been devoted to studying the propagation of detonation waves in narrow channels (for example [1–7]). In the present study, numerical simulations are conducted to investigate detonation propagation from a wider channel into a very narrow channel, both with and without wall heat losses. The width of the narrow channel is roughly 50 times smaller than the average detonation cell size of stoichiometric ethylene-air mixture [8]. To capture flow and detonation features, an adequate level of grid resolution must be used. Coarser grids are known to produce overly diffusive numerical solutions, obscuring critical detonation features such as cellular structures [4]. Insufficient refinement can give misleading results, with respect to predictions of capturing processes such as detonation propagation and quenching. This study addresses the question of how much grid resolution is required for a typical narrow channel computation, particularly focusing on accurately capturing detonation front and shock-flame decoupling inherent to narrow channel configurations.

2 Numerical Model

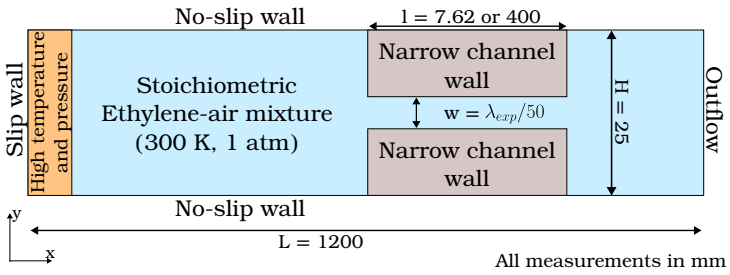

Figure 1: Computational domain with initial and boundary conditions

The numerical simulations were performed using a multidimensional, reactive-flow code AMRFCT, which has been extensively tested in multiple detonation problems [8, 9]. AMRFCT solves the unsteady, fully-compressible, reactive, Navier-Stokes equations using a fourth-order Flux Corrected Transport (FCT) algorithm. The time integration is performed explicitly using a second-order Runge-Kutta scheme

Correspondence to: milin333martin@tamu.edu

with the timestep limited by the CFL condition. Chemical heat-release of the reactive mixture is modeled using the Chemical-Diffusive Model (CDM) [8, 10, 11]. Adaptive Mesh Refinement (AMR) is used to obtain accurate solutions at the shock and reaction fronts.

Figure 1 shows the computational domain used for this study. The size of the domain is 90 x 2.5 cm ($L \times H$). The entire domain is initialized with stoichiometric ethylene-air mixture at 300 K and atmospheric pressure. The detonation is initiated by hot reactants at von Neumann pressure and temperature. The detonation in the wider channel propagates steadily at nearly the CJ speed until it reaches the narrow channel. The wider channel has a no-slip wall on the top and bottom, and an outflow boundary condition at the right end. The dimensions of the narrow channel is 100 x 0.38 mm ($l \times w$).

Multiple sets of computations are performed with the narrow channel walls that are either adiabatic or have heat loss. The wall heat loss model is based on conjugate heat transfer problem described in [12]. At the interface of the solid wall and gas, the heat flux must become identical, so that,

$$k_{fluid}\left(\frac{T_{fluid}-T_{wall}}{\Delta x}\right) = k_{solid}\left(\frac{T_{wall}-T_{solid}}{\Delta x}\right) \implies T_{wall} = \frac{T_{fluid}k_{fluid}+T_{solid}k_{solid}}{k_{fluid}+k_{solid}} \quad (1)$$

Here, (k_{fluid}, T_{fluid}) and (k_{solid}, T_{solid}) refers to the thermal conductivity and core temperature of the fluid and solid respectively. For the purpose of this study, $k_{solid} = 16.2$ W/m-K and $T_{solid} = 300$ K, corresponding to 304 stainless steel. The wall temperature (T_{wall}) is updated at each step of the computation.

Table 1: Grid resolution relative to heat-release zone distance (L_{hr})

Grid resolution	Finest grid size (μm)
$L_{hr}/8$	17.8
$L_{hr}/16$	8
$L_{hr}/32$	4
$L_{hr}/64$	2

The base grid of the domain consists of 4608 x 128 cells in the x- and y- directions, respectively. For the larger domain, the finest grid size of 28.5 μm (3 AMR levels) is used. This corresponds to 5 cells per heat-release zone distance (L_{hr}) of the ZND profile of this mixture, based on recommendations from [13]. Once the detonation wave reaches the narrow channel, computations are repeated for the four different grid resolutions shown in Table 1. The effect of grid resolution on the solutions of narrow channel detonations with and without wall-heat losses is studied. These computations were performed on the GPU nodes of the GRACE cluster. The maximum wall time for the simulation at the highest resolution was approximately 20 hours.

3 Results

3.1 Comparison of reaction front speeds

Figure 2 shows the normalized reaction front speed (S/D_{CJ}) as a function of the distance along the narrow channel. For a narrow channel with adiabatic walls, the detonation persists throughout the channel length. Upon exiting the channel, the shock and reaction front decouple, resulting in detonation quenching (Figure 2a). In contrast, for a narrow channel with wall heat losses, the detonation is quenched

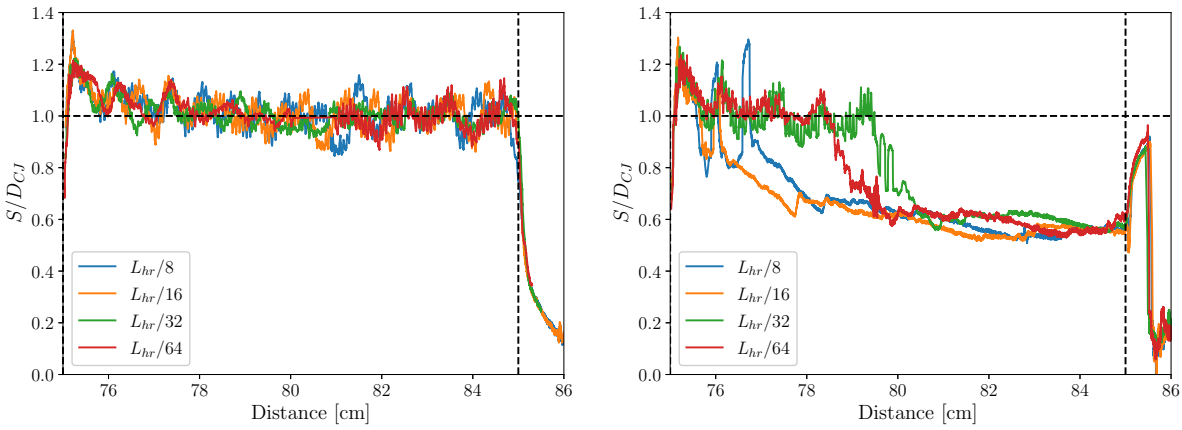

(a) Narrow channel with adiabatic walls

(b) Narrow channel with wall-heat losses

Figure 2: Effect of grid resolution on reaction front speed

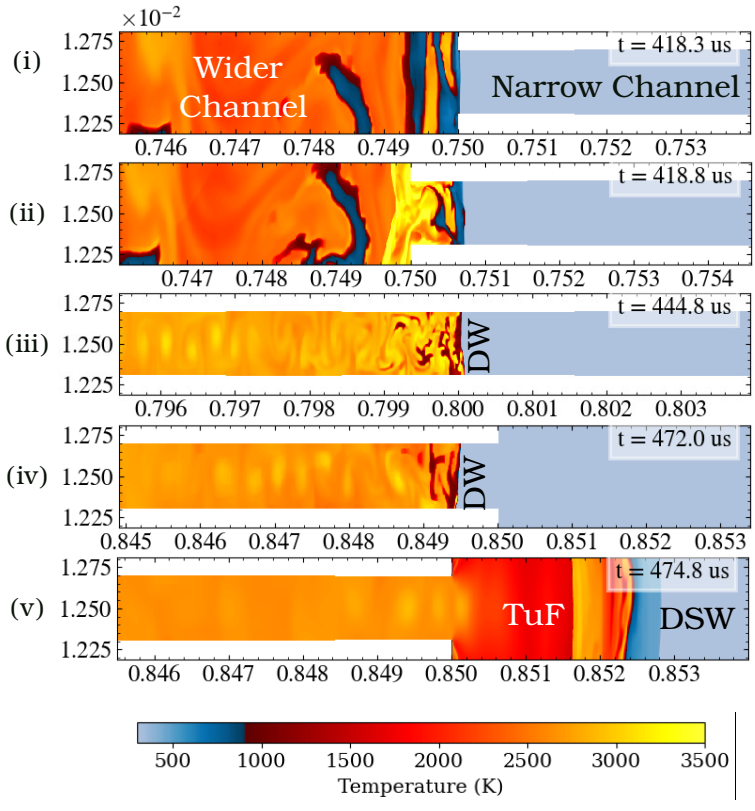

DW - Detonation Wave TuF - Turbulent Flame
DSW - Decoupled Shock Wave

Figure 3: Time series of temperature slices as the detonation propagates in the narrow channel with adiabatic walls at different grid resolution. These snapshots show: (i) CJ detonation before entry, (ii) after the detonation enters the narrow channel, (iii) detonation has propagated to the center of the channel, (iv) detonation about to exit the narrow channel, (v) after the decoupled shock and reaction waves exit the narrow channel.

within the channel, as indicated by the decrease in flame front speed (Figure 2b). With increased grid resolution, the location of this dip becomes stochastic. However, after the decoupling of the shock and reaction front, the reaction front speed stabilizes at nearly half the CJ detonation speed.

3.2 Computations of narrow channels with and without wall-heat loss

The converged solution of detonation propagating in the narrow channel with adiabatic walls and walls with heat loss are illustrated in Figure 3 and 4 respectively.

Detonation propagates in a wider channel with a near-CJ speed. Figure 3(i) shows the zoomed region close to the narrow channel without wall-heat loss, as the CJ detonation enters it. The detonation propagates with a CJ speed and does not quench throughout the length of the channel. As the detonation exits the narrow channel into a wider channel, it decouples into a turbulent flame and shock wave. Thus, the detonation is quenched at the exit.

Figure 4 shows the snapshots of temperature field for the computations of narrow channel with wall-heat losses. Similar to the previous case, a CJ detonation enters the narrow channel (Figure 4(i)). As the detonation propagates downstream, the temperature of the burned mixture near the wall decreases. Over time, the detonation weakens further, eventually leading to the decoupling of the flame front and the leading shock wave. The leading shock moves faster than the trailing flame front, widening the gap between them. The shock exits the channel first, followed by the trailing turbulent flame, which is released into the post-shock environment created by the leading shock wave.

4 Conclusions and Discussions

Increasing the grid resolution does not change the physical processes occurring inside the channel, although the locations where these processes take place become stochastic. The resolution also impacts the structure of the shock-flame complex during decoupling. Increasing the resolution from $L_{hr}/8$ to $L_{hr}/32$, more unreacted pockets of reactive mixture are resolved. Further increasing to $L_{hr}/64$ however, does not improve the detonation structure. Additionally, as the trailing flame front propagates in the narrow channel, it becomes increasingly smoother and curved with higher grid resolution.

The results presented in this work indicate that the grid resolution used outside the narrow channel is insufficient to capture salient flow and detonation features within it. For narrow channels with adiabatic walls, a resolution of 16 to 32 cells per heat-release-zone length is sufficient to resolve the detonation structure. However, resolution becomes more critical for narrow channels with wall heat losses. For these computations, a resolution of 32 to 64 cells per heat-release-zone length is necessary to resolve the structure of the shock-flame complex as the detonation gets quenched inside the channel.

Based on this work, preliminary 3D calculations of these channels have been performed using the lowest grid resolution. In these calculations, whether the walls are adiabatic or have heat loss, the detonation is quenched upon entry into the narrow channel. Detailed investigation of the 3D results will be discussed in the future.

5 Acknowledgments

This work is supported by Emerson Process Management Regulator Technologies, Inc. and the O'Donnell Foundation Professorship at Texas A&M University. We also thank the Texas A&M HPRC for providing the computational resources.

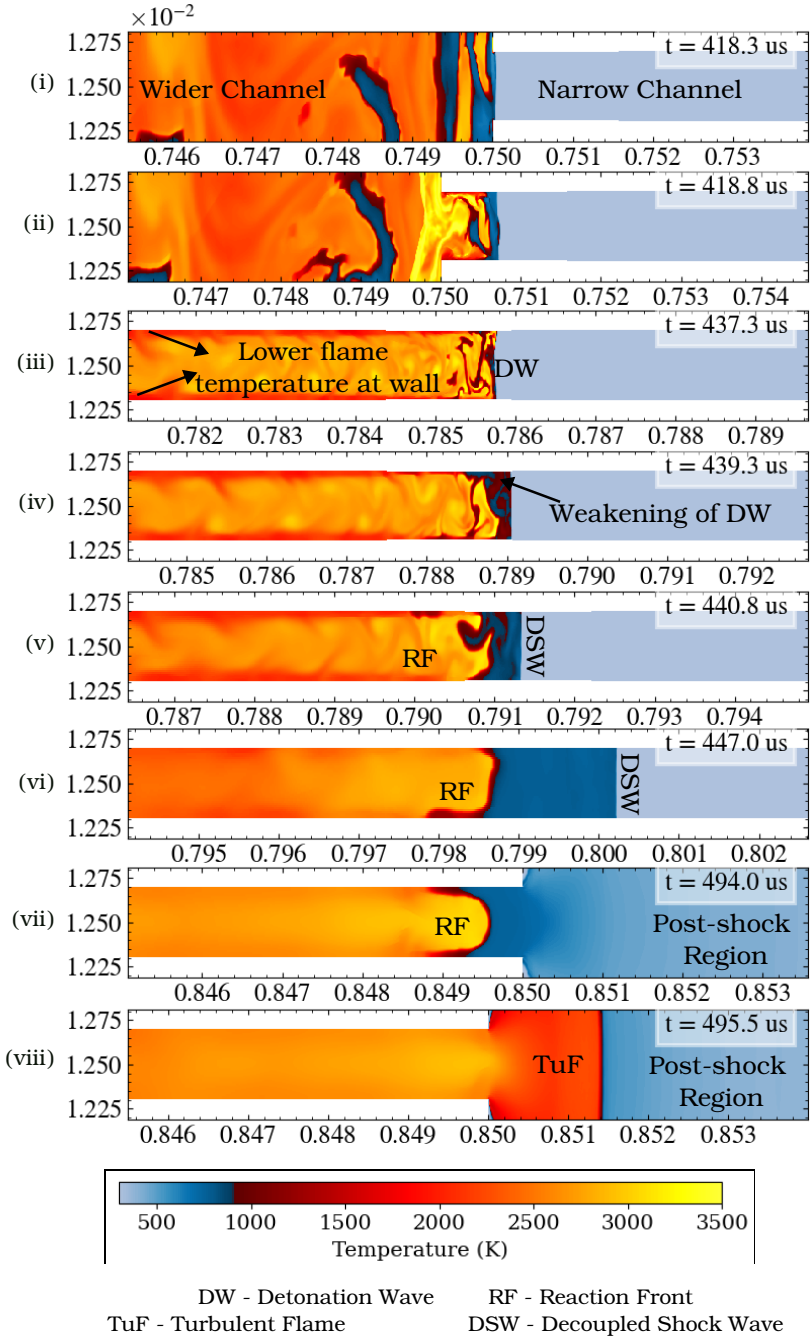

Figure 4: Time series of temperature slices as the detonation propagates in the narrow channel with wall-heat loss at different grid resolution. These snapshots show: (i) CJ detonation before entry, (ii) after the detonation enters the narrow channel, (iii) detonation propagating in the channel, (iv) onset of the decoupling of shock wave and reaction wave, (v) & (vi) flame front trailing behind a decoupled shock wave, (vi) flame front exiting to a shocked region, (viii) after the decoupled shock and turbulent flame exit the narrow channel.

References

[1] E. S. Oran, T. R. Young, J. P. Boris, J. M. Picone, and D. H. Edwards. "A study of detonation structure: The formation of unreacted gas pockets". In: *Proc. Combust. Inst.* 19.1 (1982), pp. 573–582. DOI: https://doi.org/10.1016/S0082-0784(82)80231-2.

[2] J. D. Ott, E. S. Oran, and J. D. Anderson. "A Mechanism for Flame Acceleration in Narrow Tubes". In: *AIAA Journal* 41.7 (2006), pp. 1391–1396. DOI: https://doi.org/10.2514/2.2088.

[3] M. I. Radulescu, G. J. Sharpe, J. H. S. Lee, C. B. Kiyanda, A. J. Higgins, and R. K. Hanson. "The ignition mechanism in irregular structure gaseous detonations". In: *Proc. Combust. Inst.* 30.2 (2005), pp. 1859–1867. DOI: https://doi.org/10.1016/j.proci.2004.08.047.

[4] A. Chinnaya, A. Hadjadj, and D. Ngomo. "Computational study of detonation wave propagation in narrow channels". In: *Phys. Fluids* 25.11 (2013), p. 036101. DOI: https://doi.org/10.1063/1.4792708.

[5] D. Liu, Z. Liu, and H. Xiao. "Flame acceleration and deflagration-to-detonation transition in narrow channels filled with stoichiometric hydrogen-air mixture". In: *Int J Hydrogen Energy* 47.20 (2022), pp. 11052–11067. DOI: https://doi.org/10.1016/j.ijhydene.2022.01.135.

[6] D. Jun, D. Kwon, and B. J. Lee. "Numerical study on the reinitiation mechanism of detonation propagating through double slits in a planar channel". In: *Combust. Flame* 261 (2024), p. 113271. DOI: https://doi.org/10.1016/j.combustflame.2023.113271.

[7] R. Houim, A. Ozgen, and E. Oran. "The role of spontaneous waves in the deflagration-to-detonation transition in submillimeter channels". In: *Comb. Theory and Mod.* 20.6 (2016), pp. 1068–1087. DOI: https://doi.org/10.1080/13647830.2016.1249523.

[8] A. S. Venkataraman, E. T. Balci, F. Hoden, and E. S. Oran. "Calibration of Chemical-Diffusive Model and its effects on C_2H_4-air detonation dynamics". In: *Proc. Combust. Inst.* 40.1-4 (2024), p. 105731. DOI: https://doi.org/10.1016/j.proci.2024.105731.

[9] A. S. Vekataraman and E. S. Oran. "Computational studies of the interaction of a detonation and a bow shock". In: *AIAA SCITECH 2023 Forum* 47 (2023), pp. 1–16. DOI: https://doi.org/10.2514/6.2023-0347.

[10] C. R. Kaplan, A. Ozgen, and E. S. Oran. "Chemical-diffusive models for flame acceleration and transition-to-detonation: genetic algorithm and optimization procedure". In: *Combustion Theory and Modeling* 23.1 (2018), pp. 1–20. DOI: https://doi.org/10.1080/13647830.2018.1481228.

[11] X. Lu, C. R. Kaplan, and E. S. Oran. "A chemical-diffusive model for simulating detonative combustion with constrained detonation cell sizes". In: *Combust. Flame* 230 (2021), p. 111417. DOI: https://doi.org/10.1016/j.combustflame.2021.111417.

[12] Y. Hou, M. Cheng, Z. Sheng, and J. Wang. "Unsteady conjugate heat transfer simulation of wall heat loads for rotating detonation combustor". In: *Int J of Heat and Mass Transfer* 221 (2024), p. 125081. DOI: https://doi.org/10.1016/j.ijheatmasstransfer.2023.125081.

[13] J. Y. Choi, F. H. Ma, and Y. V. "Some numerical issues on simulation of detonation cell structures". In: *Combustion, Explosion, and Shock Waves* 44 (2008), pp. 560–578. DOI: https://doi.org/10.1007/s10573-008-0086-x.